Structure of magnetite (Fe3O4) above the Curie temperature: a cation ordering study

Structure of magnetite (Fe_3O_4) above the Curie temperature: a cation ordering study.

Abstract

In order to characterize the structural and magnetic behavior of magnetite (Fe3O4) at high temperature, a sample of pure phase was studied at high temperature (273 – 1073 K) by means of Neutron Powder Diffraction. By an accurate analyzes of the collected data, the main features of the magnetite was determinate in function of the temperature. The magnetic moments of the tetrahedral and octahedral sites was extracted by the magnetic diffraction up to the Curie temperature (between 773 and 873 K). The thermal expansion presents a change of slope around the Curie temperature, moreover the oxygen coordinate increase above 700 K. These two features are due to a change in the thermal expansion of the tetrahedral site. The authors show that this anomaly is due to a cation reordering: the magnetite from a disorder configuration transform in a partially ordered one. By a simple model based on the cation-oxygen bond length, it was possible to determine the order degree in function of temperature and consequently the enthalpy and entropy of the reordering process. The refined values are ΔH^0=-23.2(1.7)kJmol^{-1} and ΔS^0=-16(2)JK^{-1}mol^{-1}. This result is in perfect agreement with the values reported by Wu (1981) and Mack (2000)

Introduction

Magnetite is the first magnetic material known since the ancient times. The structure, formally $Fe^{II}Fe^{III}_2O_4$, is spinel-like (Fleet, 1981; Fleet, 1986) and is derived from an oxygen cubic close packing with cations in the interstitial tetrahedral and octahedral sites. This kind of structure is ideally cubic and it is typical for many AB_2O_4 compounds, where A is usually a bivalent cation and B a trivalent one. Two limit-configurations are possible: in the so called ‘normal’ structure the A and B cations fill the tetrahedral and octahedral sites respectively, whereas in the ‘inverse’ one the tetrahedral sites are filled by half B cations while the residual half of B and all A cations fill disorderly the octahedral sites. The study of cation partitioning in spinels is widely used in geology to interpret the genesis of these phases in natural rocks, but it is also important to study their physical properties in material science. Magnetite is a typical inverse spinel (Verwey and Haayman, 1941) in which Fe(II) and Fe(III) are disordered in the octahedral sites, while tetrahedrons are fully occupied by Fe(III) cation. From the point of view of the magnetic properties, magnetite has a Verwey ordering at low temperature (T_v=118K) (Verwey and Haayman, 1941) and it is ferromagnetic up to the Curie Temperature, at about 856 K (L. Néel, 1948); above such value it

becomes paramagnetic (Shull et al., 1951). The ferromagnetism is due to an anti-ferromagnetism coupling of Fe(III) in tetrahedral and octahedral sites. In the last years, magnetite has become an important technological material as a nanomagnetic component (Poddar et al., 2002). Another peculiar behavior shown by magnetite has been discovered by Rozenberg et al. (2007) at high-pressure: above 20 GPa an enlargement of the tetrahedral site has been highlighted, this occurrence being possibly referred to a structural transition of this phase from *inverse* to *direct* spinel. As a matter of fact, the Fe^{2+}-O bond length is bigger than the Fe^{3+}-O bond length in tetrahedral sites - 2.03Å and 1.89Å respectively (Shannon, 1976).

An in-depth study of the structure of magnetite at high temperature is limited by the strong Fe(II) inclination to be oxidized even in presence of very small quantities of oxygen when heated above 373 K (personal observation). Despite this difficulty, some studies concerning the high temperature structural behavior of magnetite have been reported. A cation distribution study on magnetite at high temperature has been performed using the thermopower measurement (Wu and Mason, 1981), thus discovering that a partial ordering of the spinel structure starts at 585° C and proceeds until the melting temperature (1773 K) is reached. The maximum percentage of direct spinel-structure detected at the highest temperature is 35%. The same results have been reported by using Mössbauer spectroscopy (Mack et al., 2000; Wissmann et al., 1998). A structural work on magnetite at high temperature has also been made by using X-ray single crystal (Okudera et al., 1996), showing that there are no significant structural changes in magnetite below the Curie temperature; unfortunately, no data have been reported for higher temperatures. Another structural work at high temperature (Mazzocchi and Parente, 1998), performed by using neutron multiple diffraction data on a single crystal, reported the magnetite structure at 976 K but included no discussion about a possible cation partitioning. In a previous work (Levy et al., 2004), it has been stated that the thermal expansion coefficient shows a change at the Curie temperature in a slightly oxidizing environment (this effect is usually referred to as the 'lost of the magnetostriction'), whereas the same coefficient evidences no variation in a reducing atmosphere. The aim of this work is to describe the effect of the Curie magnetic transition on the structure of magnetite and to study and explain the variation of the thermal expansion coefficient at high temperature from a structural point of view.

Experimental

Sample

This study has been performed on a natural sample (S1 hereafter) collected in the Brosso mining (Ivrea, Italy). The sample has been purified from the rock matrix by means of magnetic separation. SEM-EDS chemical analyses have been performed using a Cambridge Stereoscan 360 SEM equipped Oxford INCA Energy 200 microanalysis and Pentafet EDS detector and showed the magnetite sample to be practically pure, with a maximum of 3% Mg atoms per formula unit. X-ray Powder Diffraction (XRPD) analysis, performed with a Pananalytical 'XPERT diffractometer, showed that all diffraction peaks are related to magnetite, no further impurity being detected. The calculated cell edge is a=8.3957(5) Å, in good agreement with the values reported in literature (Fleet, 1981; 1986).

Neutron Powder Diffraction data collection

The sample has been studied by means of Neutron Powder Diffraction (NPD) at high temperature; diffraction data have been collected at the Helmholtz-Zentrum, Berlin (HZB, Germany) with BER II neutron source by means of angle dispersion diffraction experiment at the E2 diffractometer.
The sample, contained in a quartz tube sample holder, has been heated *in situ* by means of a furnace in high vacuum starting from room temperature (298 K) with progressively increasing step of 100 K (except the first one, equal to 75 K) until T = 1073 K was reached. Data collection time at each temperature step was 4 hours.

Data analysis

In the collected neutron diffraction patterns, as expected, some selected peaks show a systematic intensity decrease with temperature rise (as shown in figure 1). These diffraction peaks can be related to the diffraction of magnetite magnetic structure.
NPD data have been refined using the GSAS/EXPGUI (Larson and Von Dreele, 2000; Toby, 2001) software. Peak profiles have been refined using a pseudo-Voigt function, varying the three terms Caglioti formula of the profile curve Gaussian part and the Lx and Ly parameters of the Lorentian part. Asymmetry and shift parameters have also been refined. A Shifted Chebyshev function with 20 terms has been used to interpolate the background. Two theta offset has been refined only for the room temperature diffractogram, the obtained value being used also for the other diffraction patterns.
Refinement of the structural data at room temperature, as evidenced from table 1, presents some problems. In fact the refined parameters at room temperature are not congruent with those found at

higher temperatures or with the reference diffractogram collected at room temperature by means of conventional XRPD. Main discrepancies can be summarized as follows: (i) the cell edge determined by NPD is 8.3925(5) Å vs. 8.3957(5) Å by XRPD and 8.3998(5) Å at 373 K (NPD); (ii) the magnetization moment at room temperature for the tetrahedral site is definitely not consistent with the values found at higher temperatures; (iii) the refined value of the position parameter of the oxygen atoms at room temperature is higher than the values refined in the temperature range 373-673 K. By taking into account these problems, it would seem that the room temperature neutron diffractogram may be affected by some inaccuracy that cannot be corrected *a posteriori*. In order to determine the correct value for these parameters at room temperature, the cell edge resulting from XRPD has been considered while the tetrahedral magnetic moment and the oxygen position have been extrapolated by taking into account the trend of the related curves at higher temperature.

Magnetic structure description

As expected, the intensities of the diffraction peaks are influenced by the magnetic diffraction effects. In particular, the intensity of four peaks is strongly dependent from temperature, as shown in Fig. 1: above the Curie temperature, these peaks have small or no intensity, being good markers for the magnetic-paramagnetic transition. No additional peaks have been found at all studied temperatures, so the magnetic structure of magnetite has the similar crystallographic cell to the atomic structure.

In order to describe the intensity of the magnetic diffraction peaks, a further magnetic phase has been added to the model to be refined with the Rietveld method. For such phase, a cubic cell has been used with the same cell edge of the atomic phase. To describe properly and in a simple way this magnetic structure, a F-1 symmetry has been chosen: the octahedral cations has been put in (½,½,½), (½,¾,¾), (¾,½,¾) and (¾,¾,½) and the tetrahedral atom in the same position of the atomic phase. For each atom, a unitary magnetic vector has been defined along the [111] direction; the magnetic vector for the octahedral site is anti parallel to the tetrahedral one, as showed in Fig.2.

In order to describe the variation in the magnitude of the magnetic moment a refinement of the three related components has been attempted, but the number of the magnetic diffraction peaks proved to be insufficient to obtain a stable result. To reduce the number of refined parameters, the magnetic moment components have been constrained to have the same value in the tetrahedral and octahedral sites. These restrictions allowed the magnetic peaks intensity to be refined.

Structure analysis

In the structure of magnetite, the only structural parameter that can be refined is the unique fractional coordinate of the oxygen atom. This atom, in the symmetry space group Fd3m (used to describe the magnetite structure in this work), is located on the body-diagonal of the cubic cell and its fractional coordinates (*x,y,z)* are constrained by symmetry. Table 1 lists all structural features of magnetite at each collected temperature. Together with the above mentioned position of the oxygen atom, the only other refined parameters are the isotropic displacements of both the oxygen and iron atoms and, in certain cases, the site occupancy of iron (in order to check a possible oxidation of the phase, as discussed later).

Results and discussion

Thermal expansion

The thermal expansion of the cell edge of the studied magnetite sample is reported in fig.3a, together with the thermal expansion of the cell edge of a different specimen previously collected by X-ray powder diffraction (Levy et al., 2004) under similar experimental conditions. The difference between these two curves is mainly due to different degrees of oxidation, as the sample collected with X-ray powder diffraction is reported to be slightly oxidized at the end of thermal cycle. The thermal expansion coefficients of the cell edge have also been calculated for the studied sample in each thermal stage as $\frac{\Delta a}{\mathrm{a}\Delta T}$, and the corresponding plot is reported in fig.3b: thermal expansion linearly increases with the temperature up to 673 K: above this temperature the thermal expansion strongly increases until a maximum at 873 K is reached, after the disappearing of the magnetic peaks in the diffractogram.

Magnetic refinement

The refinement of the iron atom magnetic moments has been calculated by adopting the module of the three magnetic components as described before. The resulting values are reported in table 2 and plotted in figure 4. The room temperature magnetic moments in the octahedral and tetrahedral sites are 3.75(6) μB (refined value) and 4.56 μB (extrapolated value), respectively. These results can be compared with those determined by Koltz et al. (2008) at room temperature and pressure on a synthetic sample, which indicate 3.60(6) and 4.05(4) μB for the octahedral and tetrahedral sites respectively, whereas values at higher pressure (0.7 GPa) were 3.65(6) and 4.49(9) μB. In spite of

being a little higher than those found at room temperature, both reported values are consistent with those indicated by Koltz et al. (2008) for higher pressure values (0.7) GPa. This could be explained by the fact that the sample analyzed here is natural whereas a synthetic one was used in the cited article. Another reason which might justify the reported differences could be the experienced difficulties in sharply refining this parameter due to its high sensibility to little structural variations.
The thermal evolution of the magnetic moments shows a significant decrease with temperature rise, in agreement with the decrease in intensity of the magnetic peaks as previously reported. Above 773 K the magnetic peaks in S1 disappear and the related magnetic moments cannot therefore be refined. Such a threshold indicates that the magnetite structure, as expected, does not show a magnetic order above the Curie temperature.

Structure refinement

As previously explained, the spinel structure has only one degree of freedom: the coordinate of the oxygen atom, for which all three fractional coordinates are equal. The other refined parameters are the isotropic thermal parameters of oxygen and iron ions in the related structural sites. The occupancies of iron atoms have been refined in a preliminary stage to check any possible compositional variation during heating, but in the end they have been fixed to their ideal values as no significant variation of has been found at high temperature. The values of the refined structural parameters their standard deviations and refinement error index are reported in table 1. As expected the values of the thermal parameters increase directly with the temperature rise, due to increase of the thermal motion.

A careful examination of fig.5 shows that the oxygen coordinate remains constant when temperature is below 700 K; at higher temperatures, this value begins to increase. The described behaviors for both the oxygen coordination and cell edge expansion can be explained by analyzing the dimensions of the tetrahedral and octahedral coordination polyhedrons. In figure 6, the cation oxygen bond lengths are plotted for different temperatures in the octahedral and tetrahedral sites (panel A and B respectively; notice that the scale of bond lengths on the Y axes is the same for both graphs in order to highlight the different behaviors). It has to be highlighted that below 673 K the thermal expansion of the two sites is quite similar in the two polyhedrons, whereas above this temperature the tetrahedron expansion is definitely bigger than that of octahedron. Above that temperature value, in fact, the octahedron dimension increases quite monotonically whereas the tetrahedral site shows a significant change in the thermal expansion. This behavior indicates that a temperature dependent cation reordering might occur. In fact, as already shown by Rozenberg et al. (2007), in tetrahedral coordination the Fe^{2+} has a bigger cation radius with respect to Fe^{3+} (0.63 Å

vs. 0.49 Å) (Shannon, 1976), while in the octahedral coordination the radii of the two cations are similar (0.61 Å and 0.645 Å for Fe^{2+} and Fe^{3+} respectively). Considering that the oxygen ionic radius is 1.38 Å and that, at room temperature, equal quantities of Fe^{2+} and Fe^{3+} occupy the octahedral site, we expect the Fe^{3+}-O bond length in tetrahedron to be 1.89 Å and (Fe^{2+},Fe^{3+})-O in octahedron to be 2.03 Å. These theoretical values are not too much different from those determined experimentally at room temperature (see Table 3).

Neutron diffraction cannot directly discriminate the Fe^{2+}/Fe^{3+} partitioning, having the two cations the same neutron cross section. An indirect method has therefore to be taken into account in order to evaluate how cation partitioning behaves in magnetite by means of neutron diffraction data; in this work the variation in the bond lengths has been analyzed. At high temperature, the bond length variation is due to two main causes: thermal expansion and cation partitioning. As from the above mentioned considerations on cation dimensions the tetrahedral site appears to be more sensitive to Fe^{2+}/Fe^{3+} exchange, the proposed way to determine the cation partition of iron can be summarized as follows:

1- The thermal expansion of the tetrahedron, hypothesized linear, has been determined on the basis of bond length values in the temperature range between 298 and 673 K, where the expansion is linear. Another plausible hypothesis is that such expansion does not change during the cation reordering; such an assumption can be considered sufficiently valid due to the scarce presence of the Fe^{2+} cation in the tetrahedral site.

2- The differences between the experimental bond lengths and the calculated ones using the thermal expansion values according to the procedure described in previous point 1 have been determined.

3- The values found at point 2 have been summed to the experimental bond lengths measured at room temperature, in order to possibly determine the bond lengths values at different temperatures without the thermal expansion contribution

4- A linear correlation between the tetrahedral bond length and Fe^{2+} occupancy has been hypothesized, using the following formula:

$$TBL = xF2BL + (1 - x)F3BL,$$

where *TBL* is the tetrahedral bond length determined as previously reported, F2BL is Fe^{2+}-O bond length reported in literature for the tetrahedron (Shannon, 1976), F3BL is the one for the Fe^{3+}-O bond length and *x* is the site occupancy for Fe^{2+}

5- To obtain the Fe^{2+} occupancy, the above mentioned equation has been resolved as a function of *x*: $x = \frac{(TBL - F3BL)}{(F2BL - F3BL)}$

In this way, the Fe^{2+} occupancy in the tetrahedral site has been determined for each experimental temperature stage; the obtained values have been reported in Table 4 and plotted in fig. 7. The obtained result is similar to that found by thermopower and Mössbauer technique (Wissmann et al., 1998; Wu and Mason, 1981).

In order to determine from a thermodynamic point of view the cation partitioning in magnetite, the following formula has to be considered:

$$Fe_T^{2+} + Fe_O^{3+} \Leftrightarrow Fe_O^{2+} + Fe_T^{3+}$$

where the indexes T and O are referred to the iron in the tetrahedral and octahedral sites respectively. The equilibrium constant K_{CD} is defined after Mack (2000) as:

$$K_{CD} = \frac{\lambda^2}{(1-\lambda)(2-\lambda)} = \exp\left(-\frac{\Delta G^0}{RT}\right) = \exp\left(\frac{\Delta S^0}{R}\right)\exp\left(-\frac{\Delta H^0}{RT}\right)$$

where λ is the quantity of Fe^{3+} in tetrahedral site, T the temperature in Kelvin, R the perfect gas constant and ΔG, ΔS and ΔH are the Gibbs energy, entropy and enthalpy respectively. The refined value of entropy and enthalpy for temperatures between 673 and 1073 K are ΔH^0=-23.2(1.7)kJmol^{-1} and ΔS^0=-16(2)JK^{-1}mol^{-1}. This result is in perfect agreement with the values reported by Wu (1981) and Mack (2000), thus confirming the reliability of the adopted method to evaluate the magnitude of the cation partition in magnetite by means of neutron powder diffraction.

Conclusion

The anti-ferromagnetic ordering of magnetite has been observed up to 773 K by Neutron Powder Diffraction, confirming that the Curie transition is correlated to a loss of the magnetic ordering between 773 and 873 K. For the first time, the magnetization of octahedral and tetrahedral sites for magnetite has been determined up to the Curie temperature by means of a refinement of the magnetic structure using the Rietveld method.

Above the Curie temperature, dimensions of the coordination polyhedrons change due to two main causes: the thermal expansion and the cation partitioning. The tetrahedral site has shown a more enhanced sensibility to the cation partitioning due to the fact that the bigger Fe^{2+} cation enters the tetrahedron and the smaller Fe^{3+} moves to the octahedral site: the resulting difference between the tetrahedral site occupied by Fe^{2+} and the one occupied by Fe^{3+} is of about 0.14Å. By examining the expansion of this coordination site as a function of temperature and the theoretical and experimental cation-oxygen bond length, it has been possible to determine the magnitude of the cation partitioning. Consequently, the entropy and enthalpy values have been determined. The obtained values for the thermodynamic parameters are in good agreement with the reported entropy and

enthalpy values as determined by means of direct measurements of cation partition using Mossbauer spectroscopy (Mack et al., 2000).

The huge change in the tetrahedral site dimensions has proven to be the main cause in the variation of the thermal expansion parameter with temperature above the Curie transition. This shows that the variation of thermal expansion is not due to loss of magnetostriction, but instead to cation partitioning.

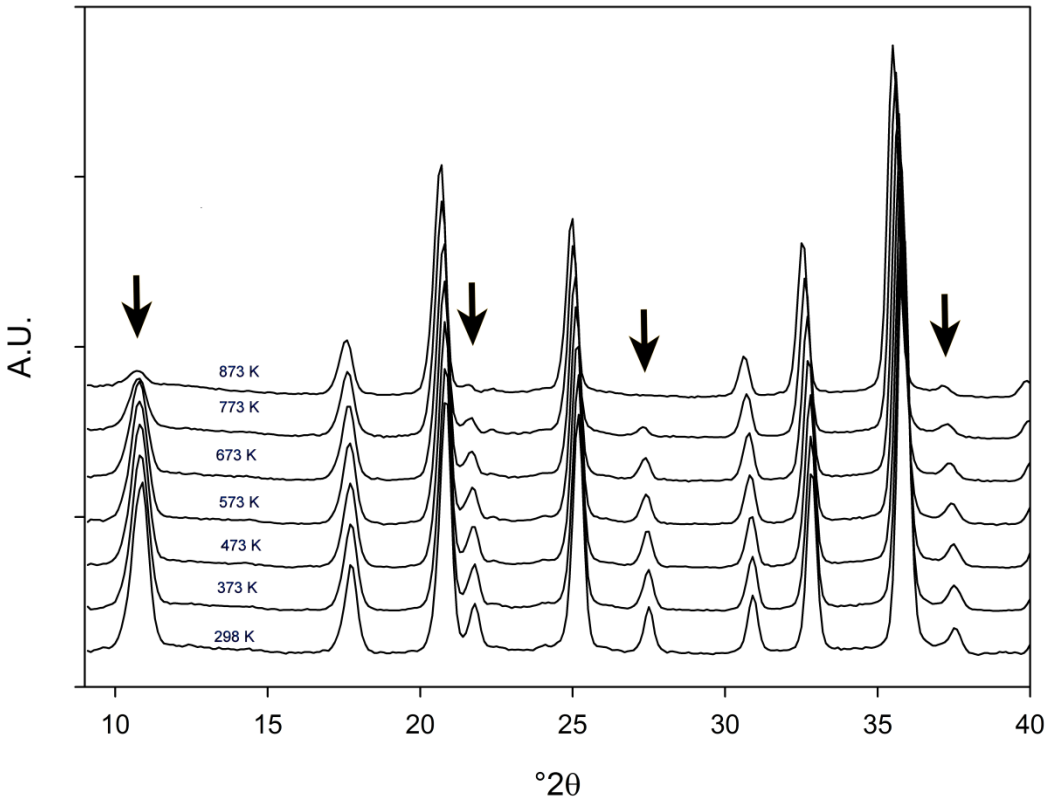

Fig1- Neutron powder diffractogram of S2 sample collected at BER II neutron source, E2 diffractometer, from 298 to 873 K. Arrows indicate the diffraction peaks which contribute the higher magnetic diffraction.

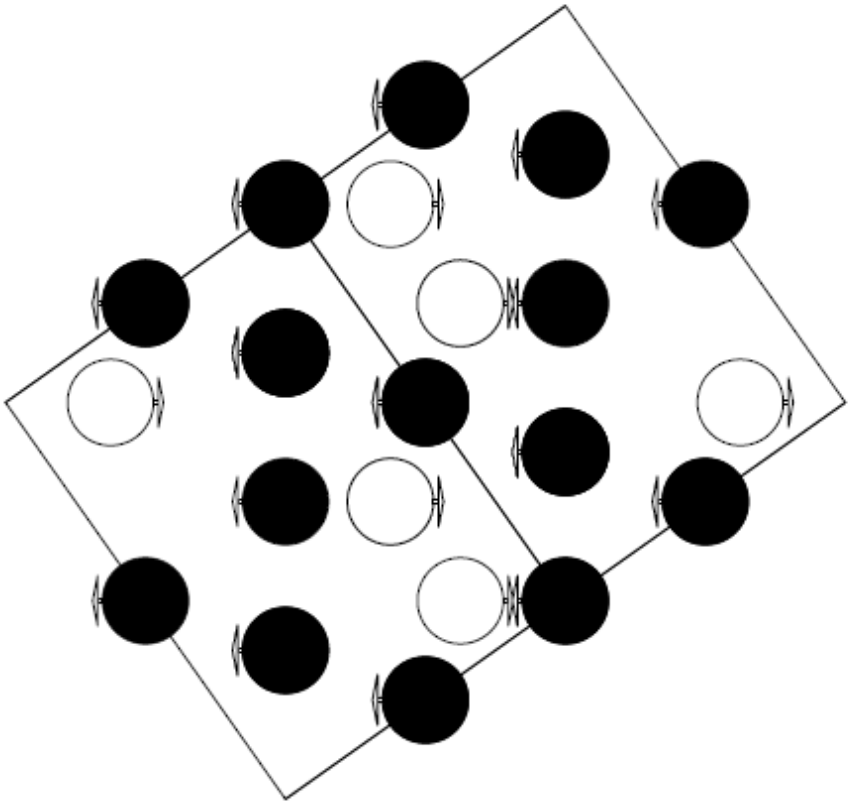

Fig.2- Magnetic structure of magnetite along the (011) plane. Black balls represent Fe in the octahedral site; white ones in the tetrahedral site.

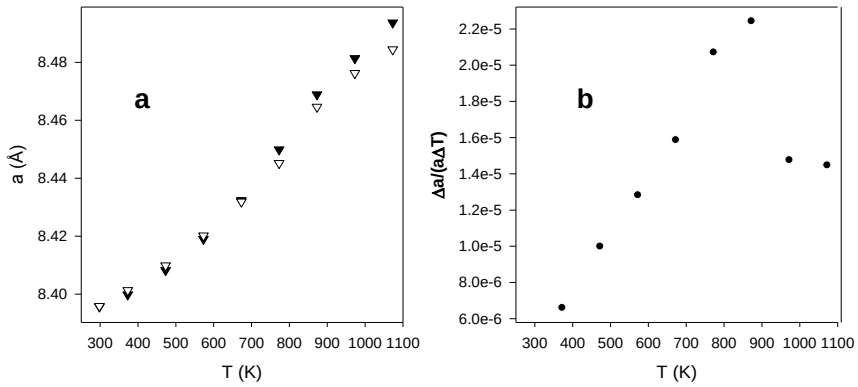

Fig 3-In panel a, the cell edge of magnetite is plotted vs. temperature; black triangles are referred to the data in this work, white triangles to data collected by means of x-ray powder diffraction (Levy et al., 2004). In panel b, the thermal expansion coefficient is plotted at different temperatures.

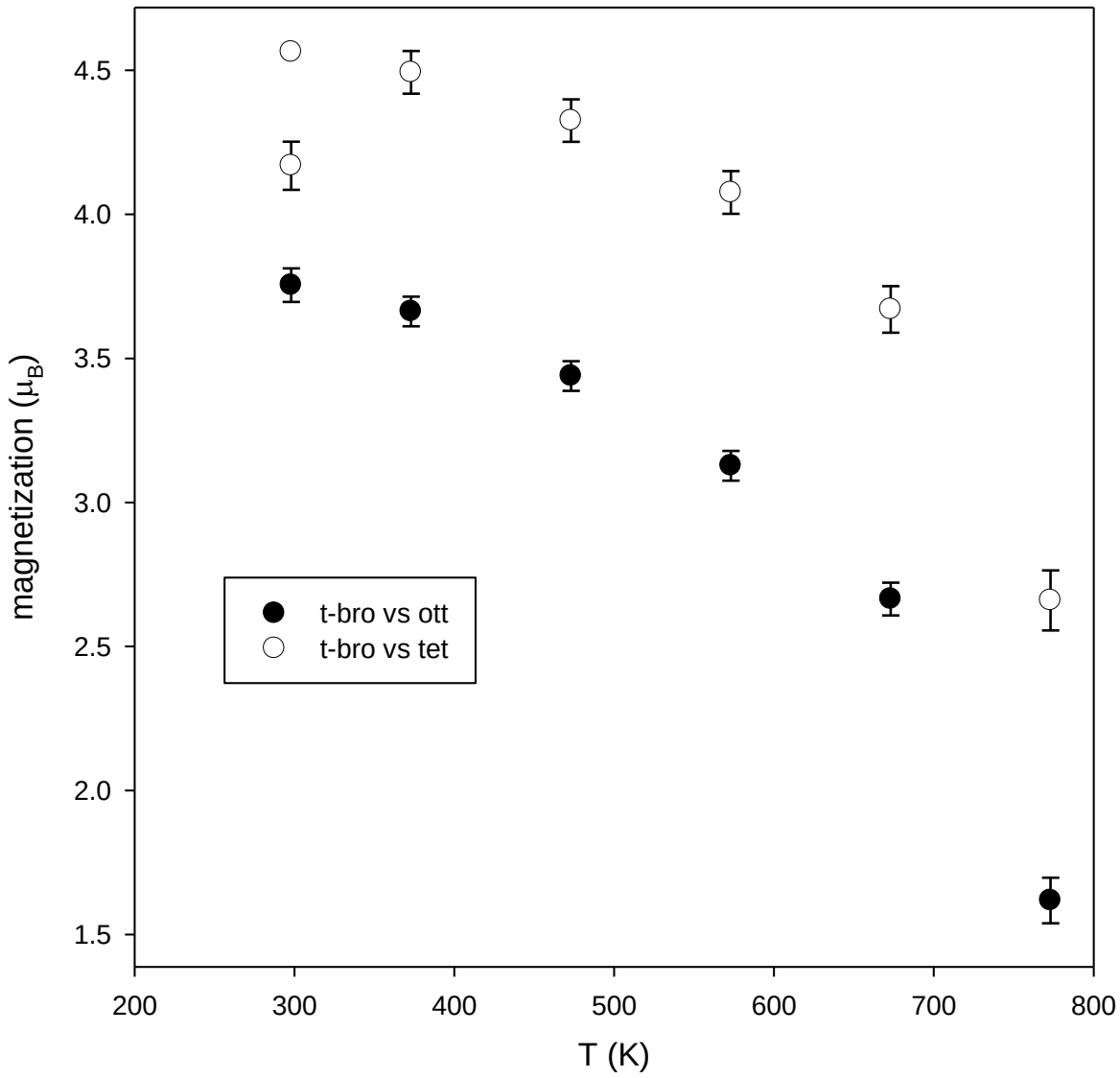

Fig.4- magnetization of Fe in the two crystallographic sites vs. temperature. The black circles represent the magnetization of the octahedral site, while the white ones that of the tetrahedral site. Note that the room temperature value of the tetrahedral magnetization has been corrected as described in the text.

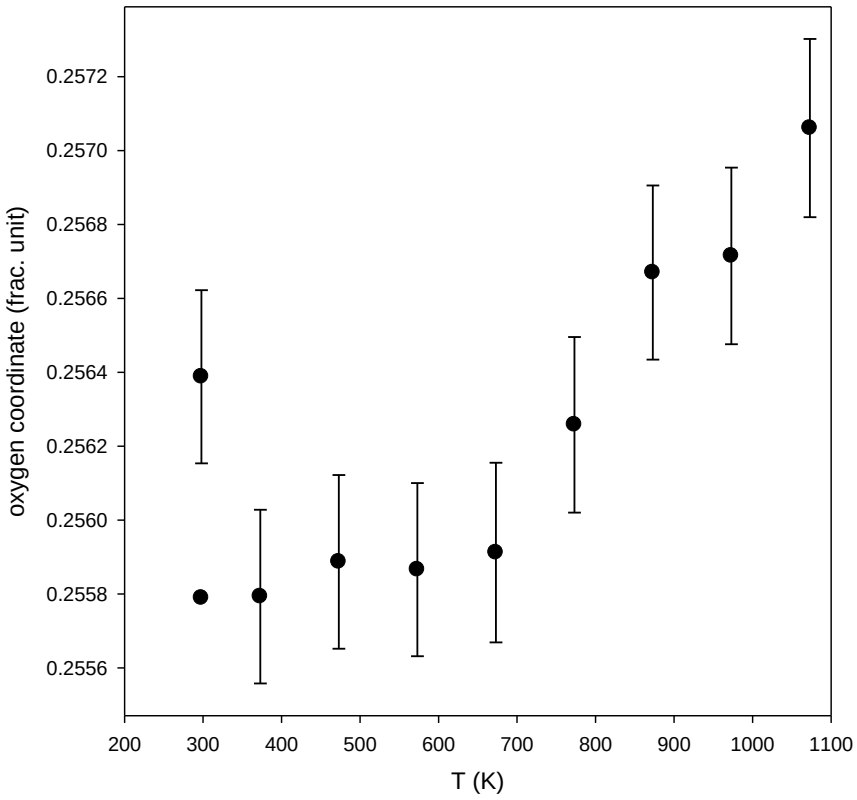

Fig.5- oxygen coordinate vs. temperature. Note that the room temperature value of the oxygen coordinate has been corrected as described in the text.

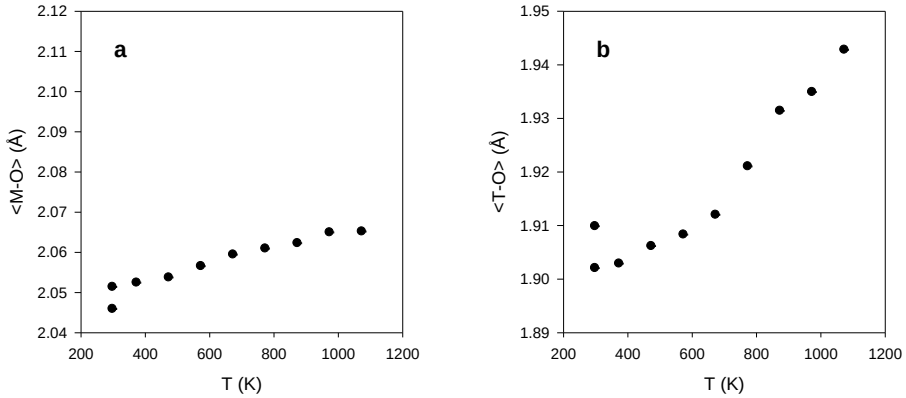

Fig.6- oxygen coordinate vs. temperature. In panel **a** the octahedral cation-oxygen bond length is plotted vs. temperature; in the panel **b** the tetrahedral one is reported. Note that the room temperature value of the oxygen coordinate has been corrected as described in the text.

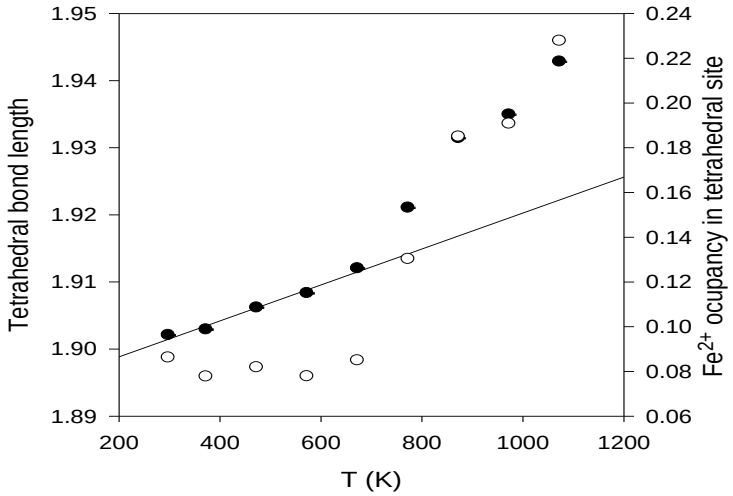

Fig.6- Black circles are the tetrahedral bond length; the continuous line is the linear regression of the tetrahedral thermal expansion computed on the first five points; white circles are the quantity of Fe^{2+} in tetrahedral coordination polyhedron.

T(K)	R_{wp}	$R(F^2)$	x (O)	U_{iso}(O)	U_{iso}(M)	U_{iso}(T)	M_x(M)	M_x(T)	a(Å)
298	5.51	3.09	0.2564(2)	0.0075(6)	0.0164(9)	0.0105(7)	2.16(6)	-2.40(8)	8.3925(5)
373	4.79	2.51	0.2558(2)	0.0100(7)	0.0130(9)	0.0107(7)	2.11(5)	-2.59(7)	8.3998(5)
473	4.57	2.36	0.2559(2)	0.0115(7)	0.0145(9)	0.0121(7)	1.99(5)	-2.50(7)	8.4082(5)
573	4.31	2.58	0.2559(2)	0.0133(7)	0.0162(9)	0.0134(7)	1.81(5)	-2.35(7)	8.4190(4)
673	4.21	2.60	0.2559(2)	0.0154(7)	0.0175(9)	0.0149(7)	1.53(6)	-2.12(8)	8.4324(5)
773	3.99	2.64	0.2563(2)	0.0177(8)	0.0202(9)	0.0169(7)	0.93(8)	-1.5(1)	8.4499(5)
873	4.07	2.28	0.2567(2)	0.0194(8)	0.0221(9)	0.0191(7)	-	-	8.4689(5)
973	3.89	2.19	0.2567(2)	0.0215(8)	0.0233(9)	0.0213(8)	-	-	8.4814(5)
1073	3.78	2.41	0.2571(2)	0.0233(8)	0.026(1)	0.0228(8)	-	-	8.4937(5)

Table 1 Refined structural features of magnetite

T (K)	$M_{ott}(\mu_B)$	$M_{tet}(\mu_B)$
298	3.75(6)	4.17(8)
298*		4.56
373	3.66(5)	4.49(7)
473	3.44(5)	4.32(7)
573	3.12(5)	4.07(7)
673	2.66(6)	3.67(8)
773	1.62(8)	2.7(1)

Table 2 Refined magnetic moment for the octahedral and tetrahedral sites

Temperature (K)	M-O (Å)	T-O (Å)
298 (calculated)	2.0459(1)	1.90992(8)
298 (extrapolated)	2.0514	1.90214(8)
373	2.0525(1)	1.90291(8)
473	2.0538(1)	1.90627(8)
573	2.0566(1)	1.90833(8)
673	2.0595(1)	1.91205(8)
773	2.0610(1)	1.92118(8)
873	2.0623(1)	1.93142(8)
973	2.0650(1)	1.93494(8)
1073	2.0652(1)	1.94282(8)

Table 3 Calculate bond lengths of cation-oxygen bonds in tetrahedral and octahedral site

T (K)	Fe2+ in tetrahedron
298	0.08
373	0.07
473	0.08
573	0.07
673	0.08
773	0.13
873	0.18
973	0.19
1073	0.22

Table 4 Fe^{2+} in tetrahedral site calculated by method described in the text

Fleet, M.E. (1981) The Structure of Magnetite. Acta Crystallographica, B37, 917-920.
-. (1986) The structure of magnetite: Symmetry of cubic spinels. Journal of Solid State Chemistry, 62(1), 75-82.
L. Néel. (1948) Propriétés magnétiques des ferrites. Ferrimagnétisme et antiferromagnétisme. Anneles des Physique, 3, 137.
Larson, A.C., and Von Dreele, R.B. (2000) General Structure Analysis System (GSAS). Report LAUR, 86-789.
Levy, D., Artioli, G., and Dapiaggi, M. (2004) The effect of oxidation and reduction on thermal expansion of magnetite from 298 to 1173 K at different vacuum conditions. Journal of Solid State Chemistry, 177(4-5), 1713-1716.
Mack, D.E., Wissmann, S., and Becker, K.D. (2000) High-temperature Mössbauer spectroscopy of electronic disorder in complex oxides. Solid State Ionics, 135(1-4), 625-630.
Mazzocchi, V.L., and Parente, C.B.R. (1998) Refinement of the Ferri- and Paramagnetic Phases of Magnetite from Neutron Multiple Diffraction Data. Journal of Applied Crystallography, 31(5), 718-725.
Okudera, H., Kihara, K., and Matsumoto, T. (1996) Temperature dependence of structure parameters in natural magnetite: Single crystal x-ray studies from 126 to 773 K. Acta Crystallographica Section B-Structural Science, 52, 450-457.
Poddar, P., Fried, T., and Markovich, G. (2002) First-order metal-insulator transition and spin-polarized tunneling in Fe3O4 nanocrystals. Physical Review B, 65(17), 172405.
Rozenberg, G.K., Amiel, Y., Xu, W.M., Pasternak, M.P., Jeanloz, R., Hanfland, M., and Taylor, R.D. (2007) Structural characterization of temperature- and pressure-induced inverse <-> normal spinel transformation in magnetite. Physical Review B, 75(2).
Shannon, R. (1976) Revised effective ionic radii and systematic studies of interatomic distances in halides and chalcogenides. Acta Crystallographica Section A, 32(5), 751-767.
Shull, C.G., Wollan, E.O., and Koehler, W.C. (1951) Neutron Scattering and Polarization by Ferromagnetic Materials. Physical Review, 84(5), 912-921.
Toby, B.H. (2001) EXPGUI, a graphical user interface for GSAS. Journal of Applied Crystallography, 34, 210-213.
Verwey, W., and Haayman, P.W. (1941) Electronic Conductivity and Transition Point of Magnetite. Physica 6(11), 979-87.
Wissmann, S., Von Wurmb, V., Litterst, F.J., Dieckmann, R., and Becker, K.D. (1998) The temperature-dependent cation distribution in magnetite. Journal of Physics and Chemistry of Solids, 59(3), 321-330.
Wu, C.C., and Mason, T.O. (1981) Thermopower Measurement of Cation Distribution in Magnetite. Journal of the American Ceramic Society, 64(9), 520-522.